Evaluation of CSA Prequalification Procedures of UHPC Materials for Bridge Construction

Zoi G. Ralli, Ph.D. – (corresponding author) Dr. Civil Engineer, PDF, Department of Civil Engineering, Lassonde School of Engineering, York University, Toronto, ON, Canada, Email: zoiralli@yorku.ca

Syed A.B. Husain, M.A.Sc.– Structural Designer, TELSTORM Corporation, Vaughan, ON, Canada, Email: syed.husain@telstorm.com

Stavroula J. Pantazopoulou, Ph.D., P.Eng. – Professor, Department of Civil Engineering, Lassonde School of Engineering, York University, Toronto, ON, Canada, Email: pantazo@yorku.ca

Emad Booya, PhD., P.Eng. - Adjunct Assistant Professor, University of Windsor, Windsor, Ontario, Canada. Email: booya@uwindsor.ca

Philip Loh, M.Eng., P.Eng. – Structural Engineer/ Design Build Lead, Facca Incorporated, Ruscom, Ontario, Canada, Email: philip@facca.com

Abstract

Canadian Bridges are particularly vulnerable to corrosion and long-term durability problems initiated by the easy fracture and delamination of concrete under combined stress and climatic exposure. UHPC is an alternative construction material that holds great promise to alleviate many of those durability and strength problems both in new construction and in retrofitting. While only recently it was considered an emerging material, UHPC is now implemented in infrastructure, necessitating full understanding of material behavior with ultimate goal to exploit its unique properties in design practices. In this study, a proprietary UHPC mix produced by DURA Canada is used to assess the material characterization techniques prescribed by Canadian Standards Association (CSA) for UHPC materials. This research serves as a case study for proof testing the repeatability and robustness of the prequalification procedures specified by the2019 CSA Standards, in light of the fact that these procedures have only been recently drafted and introduced in the Code. Additional objective is to evaluate the material's compliance with requirements for abrasion, salt scaling, absorption, chloride ion penetration, and freeze thaw resistance according to the different standards used by the Canadian Industry as well as time dependent properties such as creep, shrinkage, and coefficient of thermal expansion. Finally, this paper will present in detail the specimen preparation and testing, as well as the challenges encountered, lessons learnt and recommendations for future editions of the code.

Keywords: UHPFRC; UHPC; durability; bridges; material characterization

1. Introduction

Conventional concrete has been used mainly for reconstruction, and urban development which consists of residential and high-rise buildings, bridges, and highways. However, there is ample evidence that the combination of chemically aggressive environments, extreme climate conditions and aging, lead to a progressive deterioration of the material. Concrete infrastructure in cold climates, where exposure to freezing and use of de-icing salts is inevitable, and structures in marine environments, are prone to such extent of degradation that their service life may be dramatically decreased to almost half of the designed value(Mehta and Burrows, 2001). Nevertheless, maintenance and rehabilitation of the degraded concrete infrastructure could be more expensive than construction of new buildings, as it may exceed annually $1 and $20 billion for bridges and building, respectively (Yıldırım et al., 2018).

UHPFRC's favorable properties and durability have made them particularly attractive in Accelerated Bridge Construction (ABC), to eliminate the issues related to corrosion and to provide fast and non-disruptive bridge replacement (Shafieifar et al., 2018). However, methodologies to design with these materials are still being developed. With the exception of the French supplement to Eurocode 2 (AFNOR NF EN 13670/CN, 2013), all other countries that use advanced UHPFRC materials are still in the phase of code developments in the form of Informative (non-mandatory) documents and Annexes (e.g., in Canada, bridge design with UHPFRC was first described in Annex 8 of CSA-S6 in 2019, while Annex U of CSA A.23.1 (2019) recommends a series of pre-qualification tests for material approval, to provide a "Material Identity Card". The mixes have to be retested and revalidated every 24 months

In the present study, the performance of pre-qualification procedures adopted for characterization of UHPFRC in Canada is assessed and its limitations and challenges are identified. A Canadian-produced UHPFRC material is used as a case study in order to assess the performance of the 2019 CSA Standards. The experimental program consists of practical implementation of the durability, mechanical, and physical testing procedures needed in order to characterize the material properties; consistency of the approaches, dispersion, and applicability are investigated.

2. Materials and Mix Proportions

The studied material is a commercially available UHPFRC mix developed by Facca Inc., in collaboration with Dura Concrete Canada Inc. The binder contains general use cement, supplementary cementitious materials (SCM) such as fly ash, silica fume and slag, and lake sand with maximum grain of 600 μm. . High range water reducing (HRWR) and workability modifying (WM) admixtures were also used (Booya et al., 2010). With the exception of specimens designed for testing methods that are performed on fiberless UHPC, 0.2 mm diameter and 20 mm length brass-coated steel fibers were used for ductility at 2% per volume. The mixture proportions of the fiberless matrix with respect to cement mass are listed in Table 1.

Table 1: Mix Proportions of DURA ® UHPC with respect to the cement mass

Material	Cement	SCM	Sand	Water	HRWR	WM
DURA® UHPC	1	0.23	0.67	0.23	0.04	0.007

3. Investigation of Material Properties

3.1. Fresh Properties

The fresh properties of the material were evaluated according to ASTM C1856 ((2017). The material was considered self-compacting as the average flowability (from 6 batches, expressed as spread diameter) was 207.6 mm.

3.2. Compressive Strength, Modulus of Elasticity and Poisson's ratio

For the determination of compressive strength, at the age of 28 days, thirty-one UHPFRC cylinders with nominal dimensions of 75 mm x 150 mm were subjected to uniaxial compression at a loading rate of 1 MPa/s in accordance with ASTM C1856. The average compressive strength was 139.9 MPa.

Modulus of Elasticity and Poisson's ratio were obtained from thirty 75 mm x 150 mm UHPFRC cylinders subjected to uniaxial compression at the age of 28 days. Four foil strain gauges were installed along two diametrically opposed generating lines near the mid-height of the cylinder: two of them were placed vertically to measure longitudinal strains, and the other two horizontally to measure transverse strains. Each cylinder was loaded three times up to around 246 kN which corresponds to 40% of the compressive strength with a loading rate of 0.15 mm/min. The average Young's Modulus and Poisson's ratio were 46.6 GPa and 0.21, respectively.

3.3. Flexural Response

The flexural response was obtained by subjecting 100 mm x 100 mm x 300 mm UHPFRC prisms to four-point bending at a stepwise loading rate. Prior to 70% post-peak load, a loading rate of 0.15 mm/min was used. Then, it was increased by 0.05mm/min for the post-peak softening branch after the load dropped below 70% of peak. Figures 1(a) and 1(b) show the experimental setup, while Figure 1(c) illustrates the resistance curve of the beams. The average flexural strength was 28.57 MPa, with a corresponding midspan deflection of 1.4 mm.

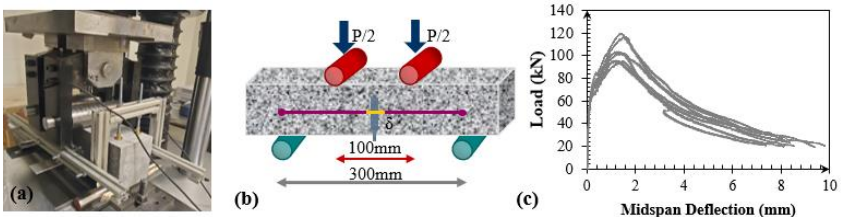

Figure 1: (a) Experimental setup; (b) geometry and schematic representation of bending test; and (c) resistance curve of 10 prisms

3.4. Tensile Response using Inverse Analysis

The resistance curves of Figure 1c were used to perform the inverse analysis procedures as prescribed in Annex 8.1 of CSA-S6 (2019). As shown in Figure 2(a), the inverse analysis essentially relies on four characteristic points of the resistance curve, which are dependent on the linearity limit and initial slope of the resistance curve (S_o). These points are used to derive a bilinear stress-strain and stress-crack width relationship (Figure 2(b)).

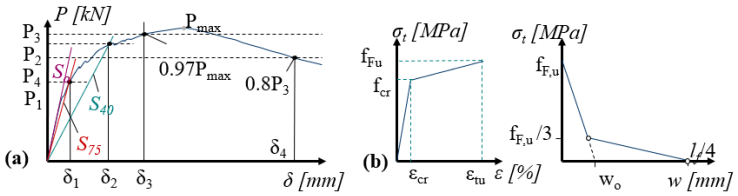

Figure 2: (a) Characteristic points of the Inverse Analysis; (b) derived tensile stress-strain and tensile stress-crack width relationship (adopted from Ralli et al., 2021).

Since the selection of S_o is entirely subjective, two inverse analyses were performed: one with the maximum estimated value of S_o and one with the minimum. The average bilinear tensile stress-strain and tensile stress-crack width law according to Annex 8.1 of CSA-S6 are illustrated in Figure 3a and 3b, respectively. As it can be seen from Table 2, the impact of choosing the minimum and maximum initial slope is significant, especially on the cracking stress and strain. These results underline a major drawback of the method which is the arbitrary selection of the initial slope.

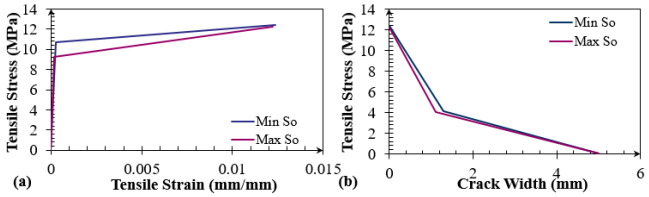

Figure 3: (a) Mean tensile stress-strain and (b) stress-crack width plots for maximum and minimum S_o

Table 2: Inverse Analysis Tensile Properties for varying initial slope S_o

Inverse Analysis Property	Min S_o	Max S_o	Difference (%)
Initial Slope S_o (kN/mm)	589.313	727.012	21.77
Cracking Tensile Strength f_{crm} (MPa)	10.74	9.22	18.70
Cracking Tensile Strain ε_{cr} (mm/mm)	0.000276	0.000186	40.70
Ultimate Tensile Strength f_{fu} (MPa)	12.40	12.24	1.41
Strain at Ultimate Strength ε_{cu} (mm/mm)	0.012364	0.012239	7.52
Crack width w_o (mm)	3.88	3.31	19.60

As a standard, the CSA prescribed inverse analysis was not found to be adequately robust in obtaining the tensile properties of UHPFRC. This is also proven by advanced computational simulations (Ralli et al., 2021) In the current development of the Annex, a different method for characterization of the material in tension is considered. The new approach quantifies the strain energy absorbed by the beam under flexure and throughout the range of the elastic and hardening part of the response. This could be considered as a minimum performance criterion for quality control of UHPFRC under flexure. The strain energy is calculated as the area under the load-deflection curve, and is proposed to be summed up until the 95% post peak load. For this batch the strain energy was 331063 Nm.

3.5. Durability Properties

3.5.1. Density, Absorption, Water, and Void content

For determination of density, absorption, water, and void content, cylinders with dimensions 75 mm x 150 mm were tested according to CSA-A.23.2 (2019). The molds were filled with a single

layer of UHPFRC. The above properties are derived using the mass of the specimens at different conditions. The low absorption (1.69 %), water (2.52%), and void content (4.26%), indicate dense microstructure and therefore high durability.

3.5.2. Abrasion Resistance

The abrasion resistance was determined as specified by Annex U, while the mass loss due to abrasion was obtained from specimens with no thermal treatment cured in 95% relative humidity at the age of 28 days. The test was performed by using a drill press with a chuck capable of holding and rotating the abrading cutter at a speed of 200 rpm, while a total force of 197±2 N was exerted on a clean flat UHPFRC surface for 2 minutes per abrasion. Three abrasion cycles were performed. As abrasion resistance among others in highly dependable on the abraded surface, and since the standard does not specify a specimen size or abraded surface. 4 different surfaces from 2 different specimens were used (Figure 5a). The results are shown in Figure b. The highest material loss is observed for the case of untreated top surface of a 150 x 150 x 150 mm cube specimen (Case A), whereas the lowest is from the same specimen, but from a formwork side (Case B). For a 100 mm diameter cylinder, the bottom surface in contact with the mold (Case C) exhibited material loss higher than expected compared to the cube, indicating that the water film that was accumulated on the mold surface caused a thin layer of porous concrete on the contact surface. The latter hypothesis was validated by cutting the cylinder half and abrading the cut surface (Case D).

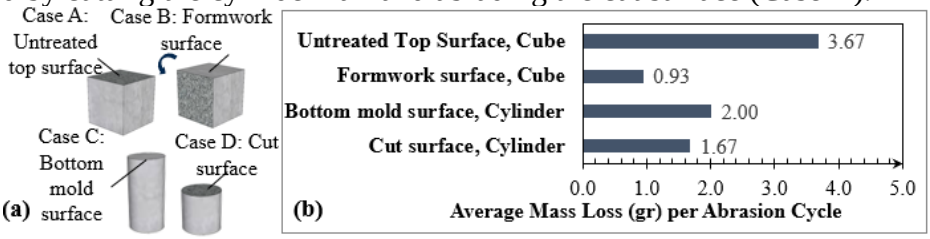

Figure 4: (a) Investigated abraded surfaces; (b) ASTM C944 Weight Loss (gr) per Abrading

3.5.3. Freeze-thaw and De-icing Salt Scaling Resistance

Freeze-thaw and de-icing salt scaling resistance are important durability properties for bridge construction in cold climates. For determination of such property three 300 mm x 300 mm x 75 mm slabs were tested according to two North American Standards, namely CSA A23.2- Annex U and ASTM C 672 (1992). The differences between these testing protocols are type and concentration of de-icing salt and testing age. For the Canadian Standard a 3% wt. NaCl solution was used, and the age of testing was 28 days, while for ASTM C 672 it was 4% wt. $CaCl_2$ solution and 56 days, respectively. Figure 5 shows the results. The visual rating specified by the Canadian Standard was 0, meaning that no significant scaling was observed after the 50^{th} cycle (Figure 5(b)). In both cases, the total abrasion was significantly below the $0.8kg/m^2$ limits, imposed by MTO. The specimen tested according to ASTM C 672 exhibited slightly higher scaling residue at every cycle. This could be attributed due the slightly higher de-icing salt concentration prescribed by the standard but mainly due to the more aggressive nature of $CaCl_2$. More specifically, it was found in the literature that the latter could result in an expansive reaction that may cause deterioration even without the freeze-thaw cycles due to the formation of calcium oxychloride at temperatures above the water's freezing point (Collepardi et al., 1994).

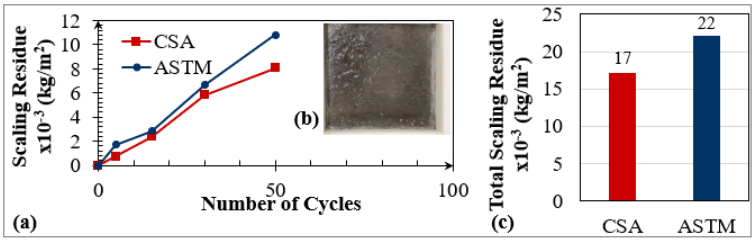

Figure 5: (a) Scaling resistance according to CSA A23.2-Annex U and ASTM C 672; (b) Visual rating of scaling after 50 cycles; (c) Total scaling residue for tests under the two standards

3.5.5. Chloride Ion Penetration Resistance

The chloride ion penetration resistance was evaluated as an electrical indication of concrete's ability to resist chloride ion penetration. Three UHPC disks of 100 mm diameter were tested using Perma2 test cells and software. The specimens which were moist cured for 56 days were fiberless to avoid short circuits. Prior to testing, the specimens were prepared by applying concrete sealer coating on the side surface and then placed in a vacuum desiccator for 18 hr. The test was conducted for 6 hrs. as described in the standard. The average charge passed was 34 Coulombs, which is considered negligible chloride ion penetration.

3.6. Time-dependent Properties

3.6.1. Shrinkage

For the assessment of shrinkage, four 75 mm x 75 mm x 295 mm UHPFRC prisms were used to the measure the length change due shrinkage. The specimens were cured for 6 days in saturated lime solution and the drying period started at the 7th day in a curing chamber with controlled conditions as prescribed by the standard. As illustrated in Figure 6, little change is observed after 28 days with an average of 0.01175% at 90 days.

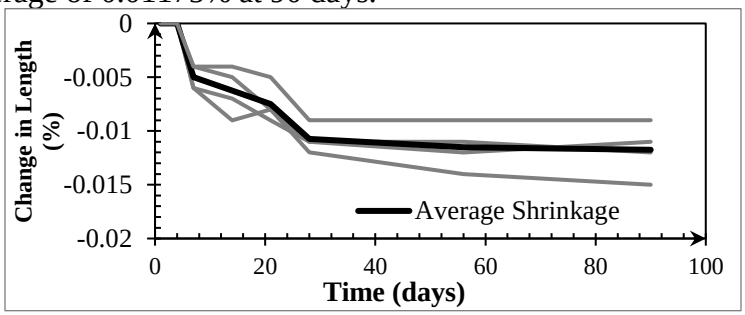

Figure 6: Change in length due to shrinkage

3.6.2. Coefficient of Thermal Expansion

To determine the Coefficient of Thermal Expansion (CTE), an adaptation of AASHTO T336((2019) is performed on 75 mm x 150 mm UHPFRC cylinders after 38 days of curing. The test was conducted at temperatures of 55 ^{o}C and 15 ^{o}C. Due to the harsh temperatures imposed by the standard, which often destroy the gauges used in this test, CTE was also evaluated in a temperature change of 21.2 ^{o}C to 3.2 ^{o}C. The average CTE for the recommended temperature range

was 16.83 x 10^{-6} while for the alternative test was 17.44 x 10^{-6} mm/mm/ºC. This value is slightly above the recommended value of 13 x 10^{-6} mm/mm/ºC by the Canadian Bridge Code but agrees with the range of values reported in the literature (Graybeal, 2006; Ahlborn et al. 2008; Semendary et al. 2019). The higher CTE value compared to conventional concrete is because this property highly depends on the CTE of the individual constituents of concrete. In case of UHPFRC, the high amount of cement and siliceous sand along with the dense microstructure result in higher CTE.

3.6.3. Creep

As per CSA Annex U, the material was also subjected to long-term creep. The specimens were moist cured for 33 days prior to testing, while the latter was performed at a sustained load of 40% of the compressive strength of UHPFRC at this age, which was 148.5 MPa. The results up to 1 year in the creep frame are shown in Figure 7.

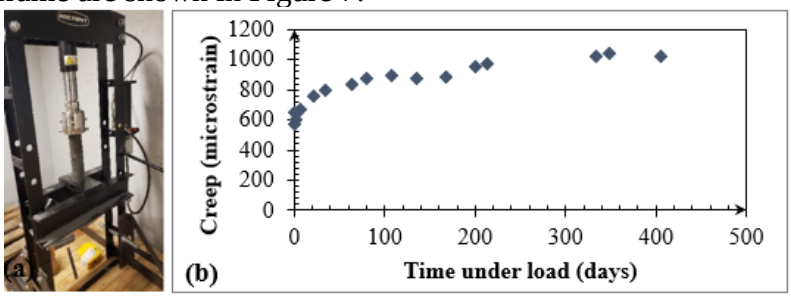

Figure 7: (a) Creep loading frame; (b) long term creep results

4. Conclusions

In this study, the performance DURA ® UHPFRC material was evaluated in terms of durability, physical and mechanical properties according to prequalification procedures prescribed by CSA A23.1/2 Annex U and CSA S6 Annex 8.1. The following conclusions can be made:

- In light of the importance of tensile properties for the UHPFRC Materials Industry, additional testing should be required where direct tension tests would be used to characterize the material. Overall, however, the current state of the art and best practices for direct tension tests also show high variance in the results needed to classify UHPFRC in tension. It is then recommended to warn CSA S6 Annex 8.1 users of this variability and to add additional methods by which UHPFRC can be classified in tension.
- Though Annex U provides durability limits, these limits for the acceptance of field testing have not yet been established due to insufficient data collection, and if they are to be provided as service design life, they should include a holistic approach not dependent on material properties
- With respect to abrasion, more specifications are needed from the standards regarding specimen size, type and abraded surface, as high dispersion was observed between different cases of abrasion in this study.
- Given the significant undertaking to complete the various tests for the Material Identity Card, it is unnecessary to retest and revalidate the mixes, if there is no major changes in the proportions and/or basic constituent material, every 24 months. We recommend

retesting and revalidating the strength properties only every 24 months, and selected durability properties every 60 months.

5. References

AASHTO T336 (2019) Standard Test Method for Coefficient of Thermal Expansion of Hydraulic Cement Concrete, , Volume 15, Washington, DC

AFNOR NF EN 13670/CN. (2013). Exécution des Structures en Béton-Complément National à la Norme NF EN1367. In *Association Française de Normalisation* . Association Française de Normalisation .

Ahlborn, M. T., Peuse, J. E., & Misson, L. D. (2008). "Ultra-High-Performance Concrete for Michigan Bridges Material Performance–Phase I". Research Report No. MDOT RC 1525. 2008

ASTM (1992). "Standard Test Method for Scaling Resistance of Concrete Surfaces Exposed to Deicing Chemicals." ASTM C 672, West Conshohocken, PA.

ASTM (2017). "Standard Practice for Fabricating and Testing Specimens of Ultra-High Performance Concrete." ASTM C1856/C1856M-17, West Conshohocken, PA.

Booya, E., Adesina, A., Loh, P., Gardonio, D., & Das, S. (2020, October). Performance of an Innovative *in-situ* Concrete Pavement Repair Patch. *2020 TAC Conference & Exhibition*, Vancouver, B.C.

CSA (2019). "Concrete materials and methods of concrete construction/Test methods and standard practices for concrete". CSA-A23.1/2:19- Annex U, Toronto, ON.

CSA (2019). " Canadian Highway Bridge Design Code (CHBDC)- Fiber Reinforced Concrete." CSA-S6 Annex 8.1, Toronto, ON.

Graybeal, B. A. (2006). "Material Property Characterization of Ultra-High Performance Concrete". Rep. No. FHWA-HRT-06-103, Federal Highway Administration, Washington, DC.

Collepardi. M., Coppola., L. and Pistolesi C. (1994). Durability of Concrete Structures Exposed to $CaCl_2$ Based Deicing Salts. *ACI Symposium Publication*, *145*.

Mehta, P. K., & Burrows, R. W. (2001). Building Durable Structures in the 21st Century. *Concrete International*, *23*, 57–63.

Ralli, Z. G., Genikomsou, A. S., & Pantazopoulou, S. J. (2021). Comparative evaluation of nonlinear FEA inverse analysis of tensile properties of UHPFRC. *Proceedings of fiv Symposium 2021 Concrete Structures: New Trends for Eco-Efficiency and Performance*

Semendary, A. A., Akentuna, M., Steinberg, E., & Hamid, W. (2019). "Influence of Heating and Cooling Temperature on the Performance of Tensile Interfacial Bond between High Strength Concrete and Ultra High Performance Concrete (UHPC). *Second International Interactive Symposium on UHPC*

Shafieifar, M., Farzad, M., & Azizinamini, A. (2018). A comparison of existing analytical methods to predict the flexural capacity of Ultra High Performance Concrete (UHPC) beams. *Construction and Building Materials*, *172*, 10–18.

Yıldırım, G., Şahmaran, M., & Anıl, Ö. (2018). Engineered cementitious composites-based concrete. In F. Pacheco-Torgal, R. E. Melchers, X. Shi, N. De Belie, K. Van Tittelboom, & A. Sáez (Eds.), *Eco-Efficient Repair and Rehabilitation of Concrete Infrastructures* (pp. 387–427)